

VLT polarimetry observations of PSR B0656+14* (Research Note)

R. P. Mignani^{1,2}, P. Moran³, A. Shearer³, V. Testa⁴, A. Słowikowska², B. Rudak⁵, K. Krzeszowski², and G. Kanbach⁶

¹ INAF - Istituto di Astrofisica Spaziale e Fisica Cosmica Milano, via E. Bassini 15, 20133, Milano, Italy

² Kepler Institute of Astronomy, University of Zielona Góra, Lubuska 2, 65-265, Zielona Góra, Poland

³ Centre for Astronomy, School of Physics, National University of Ireland Galway, University Road, Galway, Ireland

⁴ INAF - Osservatorio Astronomico di Roma, via Frascati 33, 00040, Monteporzio, Italy

⁵ Nicolaus Copernicus Astronomical Center, ul. Radańska 8, 87100, Toruń, Poland

⁶ Max-Planck Institut für Extraterrestrische Physik, Giessenbachstrasse 1, 85741 Garching bei München, Germany

Received ...; accepted ...

ABSTRACT

Context. Optical polarisation measurements are key tests for different models of the pulsar magnetosphere. Furthermore, comparing the relative orientation of the phase-averaged linear polarisation direction and the pulsar proper motion vector may unveil a peculiar alignment, clearly seen in the Crab pulsar.

Aims. Our goal is to obtain the first measurement of the phase-averaged optical linear polarisation of the fifth brightest optical pulsar, PSR B0656+14, which has also a precisely measured proper motion, and verify a possible alignment between the polarisation direction and the proper motion vector.

Methods. We carried out observations with the Very Large Telescope (VLT) to measure the phase-averaged optical polarisation degree (P.D.) and position angle (P.A.) of PSR B0656+14.

Results. We measured a P.D. of $11.9\% \pm 5.5\%$ and a P.A. of $125.8^\circ \pm 13.2^\circ$, measured East of North. Albeit of marginal significance, this is the first measurement of the phase-averaged optical P. D. for this pulsar. Moreover, we found that the P.A. of the phase-averaged polarisation vector is close to that of the pulsar proper motion ($93.12^\circ \pm 0.38^\circ$).

Conclusions. Deeper observations are needed to confirm our polarisation measurement of PSR B0656+14, whereas polarisation measurements for more pulsars will better assess possible correlations of the polarisation degree with the pulsar parameters.

Key words. Optical: stars; neutron stars: individual: PSR B0656+14

1. Introduction

Polarisation measurements of pulsars offer unique insights into their highly-magnetised relativistic environments and are a primary test for neutron star magnetosphere models and radiation emission mechanisms. Besides the radio band, optical observations are best suited to these goals. Indeed, significant polarisation is expected when the optical emission is produced by synchrotron radiation in the neutron star magnetosphere. Owing to their faintness linear optical polarisation measurements exist for a handful of pulsars only, whereas the circular polarisation was measured only for the Crab pulsar (Wiktorowicz et al. 2015). The young (~ 960 year old) and bright ($V \sim 16.5$) Crab pulsar (PSR B0531+21) is the only one for which precise measurements have been repeatedly obtained, both phase-resolved (e.g., Słowikowska et al. 2009) and phase-averaged (e.g., Moran et al. 2013). Interestingly, the phase-averaged optical polarisation position angle is similar to that of the pulsar proper motion direction and close to that of the axis of symmetry of the X-ray arcs and jets of the pulsar-wind nebula

(PWN) observed by *Chandra* (e.g. Hester 2008), which is assumed to be also the pulsar spin axis. Such an approximate alignment, might trace the connection between the pulsar magnetospheric emission, its dynamical interaction with the PWN, and the neutron star formation, with the kick and spin axis directions determined at birth. Evidence of a similar alignment has been found from optical polarisation measurements of the Vela pulsar (PSR B0833–45; $V \sim 23.6$) by Mignani et al. (2007) and Moran et al. (2014), whereas for both PSR B0540–69 ($V = 22.5$) and PSR B1509–58 ($R=25.7$) the lack of a measured proper motion makes it impossible to check the alignment with the polarisation direction (Mignani et al. 2010; Lundqvist et al. 2011; Wagner & Seifert 2000). The next best target is PSR B0656+14, the brightest pulsar detected in the optical after Vela (Mignani 2011). PSR B0656+14 ($V \sim 25$) is a middle-aged ($\sim 10^5$ years) optical pulsar (Shearer et al. 1997; Kern et al. 2003; Kargaltsev & Pavlov 2007) with strong magnetospheric optical emission (e.g., Zharikov et al. 2007). It is not embedded in a bright and variable optical PWN and its supernova remnant (SNR) has already faded away in the interstellar medium (ISM), which minimises the local background polarisation. Moreover, at a distance of 0.28 ± 0.03 kpc (Verbiest et al. 2012), PSR B0656+14 is affected by a relatively low foreground polarisation. Last

Send offprint requests to: R. P. Mignani; mignani@iasf-milano.inaf.it

* Based on observations collected at ESO, Paranal, under Programme 090.D-0106(A)

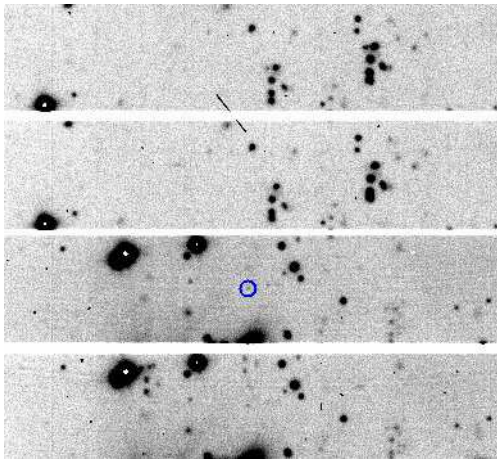


Fig. 1: Image of the PSR B0656+14 field (715 s) taken with the 0° retarder plate angle. The pair of images ($22''$ height) correspond to the extraordinary and ordinary beams. The pulsar counterpart is circled.

but not least, it has an extremely accurate radio proper motion ($\mu = 44.13 \pm 0.63 \text{ mas yr}^{-1}$; Brisken et al. 2003), which makes it possible to search for a possible alignment with the phase-averaged polarisation direction.

Here, we report on the first phase-averaged linear polarisation observations of PSR B0656+14, performed with the Very Large Telescope (VLT).

2. Observations and Data Analysis

We observed PSR B0656+14 between January and February 2014 using the second version of the Focal Reducer and low dispersion Spectrograph (FORs; Appenzeller et al. 1998) at the VLT Antu telescope. FORs2 is equipped with a mosaic of two $4\text{k} \times 2\text{k}$ MIT CCDs aligned along the Y axis, optimised for wavelengths longer than 6000 \AA . Observations were performed in imaging polarimetry mode (IPOL), with standard low gain, normal readout (200 Kpix/s), standard-resolution mode ($0''.25/\text{pixel}$), and the high efficiency v_{HIGH} filter ($\lambda = 555.0 \text{ nm}$, $\Delta\lambda = 61.6 \text{ nm}$). For all the observations, the target was at the nominal aim position on the upper CCD chip (CHIP1), to avoid the effects of instrumental polarisation at the CCD edges. The FORs2 polarisation optics consist of a Wollaston prism as a beam splitting analyser and two super-achromatic phase retarder 3×3 plate mosaics installed on rotatable mountings that can be moved in and out of the light path. Images are obtained by taking two frames displaced by $22''$ in the direction perpendicular to the Multi-Object Spectrograph (MOS) slitlets. We used the four standard IPOL half-wave retarder plate angles of 0° , 22.5° , 45° , and 67.5° , corresponding to the retarder plate orientation with respect to the Wollaston prism and usually set with an accuracy $\lesssim 0.1^\circ$ (Boffin 2014). Both the axis of the detector optics and the zero point of the half wave retarder plate angle are set such that the polarisation position angle is measured eastward from North.

In order to not introduce spurious effects due to the variable sky polarisation background across different nights, each of the nine observation blocks (OBs) incorporated exposures for all the four retarder plate angles (715 s each). Observations were executed in dark time, with a seeing of

$0''.6\text{--}1''.3$, airmass below 1.4, and in clear sky conditions. Short exposures ($< 3 \text{ s}$) of both polarised and unpolarised standard stars were also acquired for calibration. Twilight flat-field images with no retarder plate along the light path were also acquired on the same nights as the science images. For both the pulsar and standard stars, single-exposure raw images were bias-subtracted and flat-fielded using standard routines in IRAF¹. We computed the FORs2 astrometry using stars from the Guide Star Catalogue 2 (GSC-2; Lasker et al. 2008) as a reference. After accounting for all uncertainties (star centroids, GSC-2 absolute coordinate accuracy) our astrometric solution turned out to be $\lesssim 0''.1$ rms. PSR B0656+14 (Fig. 1) is detected at the position expected by extrapolating its proper motion (Brisken et al. 2013) to the epoch of our observations, where the uncertainty on the proper motion extrapolation is well below that on our astrometry calibration.

In order to increase the signal-to-noise, we co-added all the nine reduced science images of PSR B0656+14 taken with the same retarder plate angle. For each angle, we aligned the single images using the IRAF tasks `ccdmap` and `ccdtrans`, with an average accuracy of a few hundreds of a pixel. We applied the image co-addition with the routine `combine` and filtered cosmic ray hits using the `pclip` algorithm. Then, we measured the pulsar flux in each of the four co-added image through PSF photometry using the package `daophot` (Stetson 1994) implemented in IRAF. In particular, we fitted the model PSF to the pulsar intensity profile within an area of 10 pixel radius ($2''.5$), estimated from the growth curves of reference stars. We measured the sky background in an annulus of inner radius of 10.5 pixels and width of 10 pixels ($2''.6$ and $2''.5$), respectively, centred on the pulsar position. We carefully tailored this annulus both to avoid the wings of the pulsar intensity profile and accurately sample the sky background without being sensitive to strong fluctuations and gradients in the background level. We corrected the pulsar flux for the atmospheric extinction using, for each image, the average airmass value and extinction coefficients in the v_{HIGH} filter². We followed Fossati et al. (2007) to compute the errors in P.D. and P.A. From the observations of the polarised standards, the absolute calibration of our polarimetry is accurate to $\sim 0.1\%$ in P.D. and to $\lesssim 0.5^\circ$ in P.A., whereas from the observations of the unpolarised standards we found no evidence of significant instrumental polarisation at the CHIP1 aim position and no systematic deviations in the zero point of the retarder half wave plate angle. For the photometry parameters defined above, we measured a P.D. = $11.9\% \pm 5.5\%$ and a P.A. = $125.8^\circ \pm 13.2^\circ$, where the associated errors account both for statistical errors and calibration uncertainties.

3. Discussion

Although of marginal significance ($\sim 2.2\sigma$), but still comparable to those obtained for other pulsars (Mignani et al. 2007; Lundqvist et al. 2011), ours is the first and only measurement of the phase-averaged optical polarisation degree of PSR B0656+14 obtained so far. Indeed, no value of the

¹ IRAF is distributed by the National Optical Astronomy Observatories, which are operated by the Association of Universities for Research in Astronomy, Inc., under cooperative agreement with the National Science Foundation.

² www.eso.org/qc

phase-averaged polarisation was reported from the phase-resolved polarimetry observations of Kern et al. (2003). Their measurements show that the bridge between the two peaks of the optical light curve seems to be strongly polarised (P.D. $\approx 100\%$), whereas the peaks seem to be unpolarised (P.D. $\approx 0\%$). However, the large errors ($\pm 40\%$ at 1σ) attached to the phase-resolved polarisation values in each phase bin strongly affect the significance of their result. Nonetheless, such a large variation of the P.D. would suggest that the phase-average value obtained from their data would be quite low and, possibly, close to our value.

We also obtained a first measurement of the P.A. of the phase-averaged optical polarisation of PSR B0656+14. The value ($125.8^\circ \pm 13.2^\circ$) is close to the P.A. of the pulsar proper motion ($93.12^\circ \pm 0.38^\circ$; Brisken et al. 2003). Since the difference between the two angles is within 3σ , an alignment between the two vectors is possible, as clearly seen in the Crab pulsar (Moran et al. 2013) and, approximately, also in the Vela pulsar (Moran et al. 2014). Evidence of alignment between the polarisation and proper motion vectors is also found in radio (Johnston et al. 2005; Noutsos et al. 2012). For PSR B0656+14, radio polarisation measurements at 3.1 GHz give a P.A. of $-86^\circ \pm 2^\circ$ (Johnston et al. 2007) at the phase of closest approach of the magnetic pole to the observer's line of sight. This value is very close (mod 180°) to the proper motion P.A. and, accounting for the phase-dependent variations of the radio polarisation P.A. and the measurement uncertainties, is comparable to our phase-averaged optical polarisation P.A. Assuming that the pulsar proper motion vector is always aligned with the spin axis (e.g., Lai et al. 2001; Johnston et al. 2005, 2007; Noutsos et al. 2012), the alignment with the optical polarisation direction might be explained by a similar optical emission geometry and inclination angle α of the magnetic axis with respect to the spin axis for the Crab and Vela pulsars and PSR B0656+14. This is suggested by their two-peak optical light curves and possibly similar values of α (e.g. Johnston et al. 2005; McDonald et al. 2011; Zhang & Jiang 2006). For both the Crab and Vela pulsars, the phase-averaged optical polarisation and proper motion vectors are also approximately aligned with the axis of symmetry of their X-ray PWNe, thought to coincide with the pulsar spin axis. Unfortunately, for PSR B0656+14 only a tentative evidence of an X-ray PWN has been found so far (Pavlov et al. 2002).

With our VLT measurement, linear polarisation values have now been obtained for all the five brightest pulsars identified in the optical (Mignani 2011). Table 1 summarises all the measurements obtained from phase-averaged imaging polarimetry. From a general standpoint, these data suggest that the pulsar phase-averaged polarisation is lower in the optical than in radio (e.g., Weltevrede & Johnston 2008). This might be ascribed to the difference between incoherent and coherent radiation emission mechanisms in the optical and in radio, respectively. Such a comparison, however, must be taken with due care since the radio band is much broader than the optical one and the radio P.D. is frequency-dependent. In particular, it decreases from the MHz to the GHz frequency ranges, probably due to de-polarisation effects produced by scattering of the radio waves in the ISM (e.g., Noutsos et al. 2009). X and γ -ray polarisation measurements could confirm that the polarisation level depends on the underlying emission mechanisms. We investigated possible correlations between the phase-

averaged optical P.D. and the pulsar characteristic age τ , the spin period P_s and its derivative \dot{P}_s , the spin-down power \dot{E} , and the pulsar magnetic field measured both at the surface (B_s) and at the light cylinder (B_{LC}). For both the Crab and Vela pulsars, we assumed the recent *HST* measurements (Moran et al. 2013; 2014) as a reference. We did not include the VLT polarisation measurements of PSR B0540–69 and PSR B1509–58 (Wagner & Seifert 2000), which have no associated errors. The linear fit shows some evidence of a possible increase of P.D. with τ (Fig. 2a; reduced $\chi_r^2 = 0.38$). Possible trends for an increase of P.D. with P_s (Fig. 2b; $\chi_r^2 = 0.84$) and for a decrease of P.D. with \dot{P}_s (Fig. 2c; $\chi_r^2 = 0.33$) are also found. The data also suggest a possible decrease of P.D. with \dot{E} (Fig. 2d; $\chi_r^2 = 0.58$). Incidentally, we note that the opposite trend is observed in radio, as found, e.g. by observations at 4.9 GHz (von Hoensbroech et al. 1998) and 1.5 GHz (Weltevrede & Johnston 2008), although such a trend is more clear at high radio frequencies. Since the optical luminosity scales with \dot{E} (e.g., Mignani et al. 2012), the trend in Fig. 2d would also imply that the fainter pulsars are more strongly polarised than the brighter ones. On the other hand, there is no correlation between the optical P.D. and B_s (Fig. 2e; $\chi_r^2 = 14.5$), whereas a possible trend for a decrease of P.D. with B_{LC} is more apparent (Fig. 2f; $\chi_r^2 = 0.65$). To summarise, if our measurement of the PSR B0656+14 polarisation were confirmed the general picture that would emerge would be that the P.D. tends to be higher in older and less energetic pulsars, and with the lower value of the magnetic field at the light cylinder. The relatively lower values of P. D. for younger and more energetic pulsars might be due to the optical emission coming from spatially extended regions of the magnetosphere (and possibly forming caustic-like structures). In such a case, the resulting intrinsic P. D. would be lower due to effective depolarisation of the radiation from different emitting regions. The emitting regions (related to outer gaps or slot gaps) might shrink in radial extension as the pulsar ages and becomes less energetic. More optical polarisation measurements covering larger ranges in the parameter space, together with the confirmation of the uncertain ones, will assess the reality of the observed trends and link them to the pulsar physical properties.

Acknowledgements. This work is dedicated to the memory of our dear friend and colleague, Prof. Janusz Gil. We are indebted to S. Bagnulo and A. Stinton for their help in the observations planning and data analysis. RPM thanks the European Commission Seventh Framework Programme (FP7/2007-2013) for their support under grant agreement n.267251. PM is grateful for his funding from the Irish Research Council (IRC). BR acknowledges support by the National Science Centre grant DEC- 2011/02/A/ST9/00256. AS and KK acknowledge the Polish National Science Centre grant DEC-2011/03/D/ST9/00656. We thank the referee for his/her constructive review of our manuscript.

References

- Appenzeller, I., Fricke, K., Fürtig, W., et al., 1998, *The Messenger*, 94, 1
- Brisken, W.F., Thorsett, S. E., Golden, A., Goss, W. M., 2003, *ApJ*, 593, 89
- Boffin H.M.J., *The FORS2 User Manual*
- Fossati, L., Bagnulo, S., Mason, E., Landi Degl'Innocenti, E., 2007, in *The Future of Photometric, Spectroscopic, and Polarimetric Standardization*, ASP Conf. Series, 364, 503
- Johnston, S., Hobbs, G., Vigeland, S., et al., 2005, *MNRAS*, 364, 1397
- Johnston, S., Kramer, M., Karastergiou, A., et al., 2007, *MNRAS*, 381, 1625

Table 1: Summary of the phase-average linear polarisation measurements for pulsars detected in the optical. For the Crab, a value of the polarisation was obtained from phase-resolved observations by Słowikowska et al. (2009; 2012).

Pulsar	τ (10^3 yr)	P_s (s)	\dot{P}_s (10^{-13} s s $^{-1}$)	\dot{E} (10^{38} erg cm $^{-2}$ s $^{-1}$)	B_S (10^{12} G)	B_{LC} (10^5 G)	P.D. (%)	References
B0531+21	1.24	0.033	4.22	4.6	3.78	9.80	5.2±0.3	(1)
B0540−69	1.67	0.050	4.79	1.5	4.98	3.62	5.5±0.1	(2)
							5.0±2.0	(3)
							16.0±4.0	(4)
							≈5.0	(5)
							10.4	(5)
B1509−58	1.56	0.151	15.3	0.17	15.40	0.42	10.4	(5)
B0833−45	11.3	0.089	1.25	0.069	3.38	0.44	8.1±0.7	(6)
							9.4±4	(7)
							8.5±0.8	(5)
B0656+14	111	0.384	0.55	0.00038	4.66	0.007	11.9±5.5	this work

(1) Moran et al. (2013); (2) Słowikowska et al. (2012); (3) Lundqvist et al. (2011); (4) Mignani et al. (2010); (5) Wagner & Seifert (2000); (6) Moran et al. (2014); (7) Mignani et al. (2007)

Hester, J. J., 2008, *ARA&A*, 46, 127
Kargaltsev, O. & Pavlov, G. G., 2007, *Ap&SS*, 308, 287
Kern, B., Martin, C., Mazin, B., Halpern, J. P., 2003, *ApJ*, 597, 1049
Lai, D., Chernoff, D. F., Cordes, J. M., 2001, *ApJ*, 549, 1111
Lasker, B. M., Lattanzi, M. G., McLean, B. J., et al., 2008, *AJ*, 136, 735
Lundqvist, N., Lundqvist, P., Björnsson, C.-I., et al., 2011, *MNRAS*, 413, 611
McDonald, J., O'Connor, P., de Burca, D., Golden, A., Shearer, A., 2011, *MNRAS*, 417, 730
Mignani, R. P., Bagnulo, S., Dyks, J., Lo Curto, G., Słowikowska, A., 2007, *A&A*, 467, 1156
Mignani, R.P., Sartori, A., de Luca, A., et al., 2010, *A&A*, 515, 110
Mignani, R.P., 2011, *ASpR*, 47, 1281
Mignani, R.P., De Luca, A., Hummel, W., et al., 2012, *A&A*, 544, 100
Moran, P., Shearer, A., Mignani, R.P., et al., 2013 *MNRAS*, 433, 2564
Moran, P., Mignani, R.P., Shearer, A., 2014, *MNRAS*, 445, 835
Noutsos, A., Karastergiou, A., Kramer, M., Johnston, S., Stappers, B. W., 2009, *MNRAS*, 396, 1559
Noutsos, A., Kramer, M., Carr, P., Johnston, S., 2012, *MNRAS*, 423, 2736
Pavlov, G. G., Zavlin, V. E., Sanwal, D., 2002, in *Neutron Stars, Pulsars, and Supernova Remnants*, MPE Report 278, 273
Shearer, A., Redfern, R. M., Gorman, G., et al., 1997, *ApJ*, 487, L181
Słowikowska, A., Kanbach, G., Kramer, M., Stefanescu, A., 2009, *MNRAS*, 397, 103
Słowikowska, A., Mignani, R.P., Kanbach, G., Krzeszowski, K., 2013, in *Electromagnetic Radiation from Pulsars and Magnetars*, ASP Conf. Series, 466, 37
Stetson, P.B., 1994, *PASP*, 106, 250
Verbiest, J. P. W., Weisberg, J. M., Chael, A. A., Lee, K. J., Lorimer, D. R., 2012, *ApJ*, 755, 39
von Hoensbroech, A., Kijak, J., Krawczyk, A., 1998, *A&A*, 334, 571
Wagner, S. J., & Seifert, W., 2000, in *Pulsar Astronomy - 2000 and Beyond*, ASP Conf. Series, 202, 315
Weltevrede, P. & Johnston, S., 2008, *MNRAS*, 391, 1210
Wiktorowicz, S., Ramirez-Ruiz, E., Illing, R. M. E., Nofi, L., 2015, *AAS Meeting #225*
Zhang, L., Jiang, Z.J., 2006, *A&A* 454, 537
Zharikov, S., Mennickent, R. E., Shibanov, Yu., Komarova, V., 2007, *Ap&SS*, 308, 545

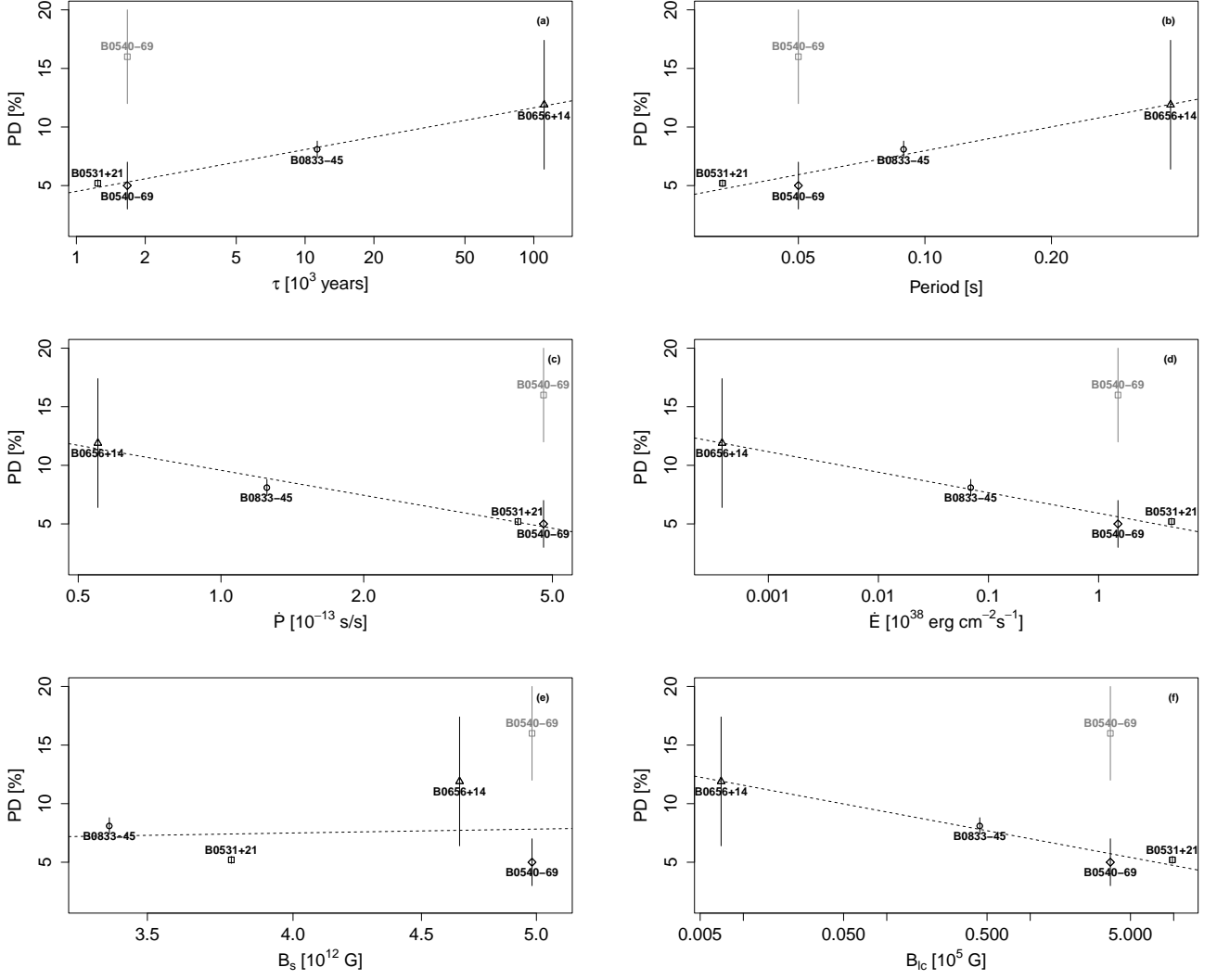


Fig. 2: Plots of the P.D. as a function of a) the pulsar characteristic age τ , b) spin period P_s , c) spin period derivative \dot{P}_s , d) spin-down power \dot{E} , e) magnetic field at the surface B_s , and f) at the light cylinder B_{LC} . The dotted lines show the best fit to the points with a linear function. The point in light grey deviates more than 1σ from the best fit.